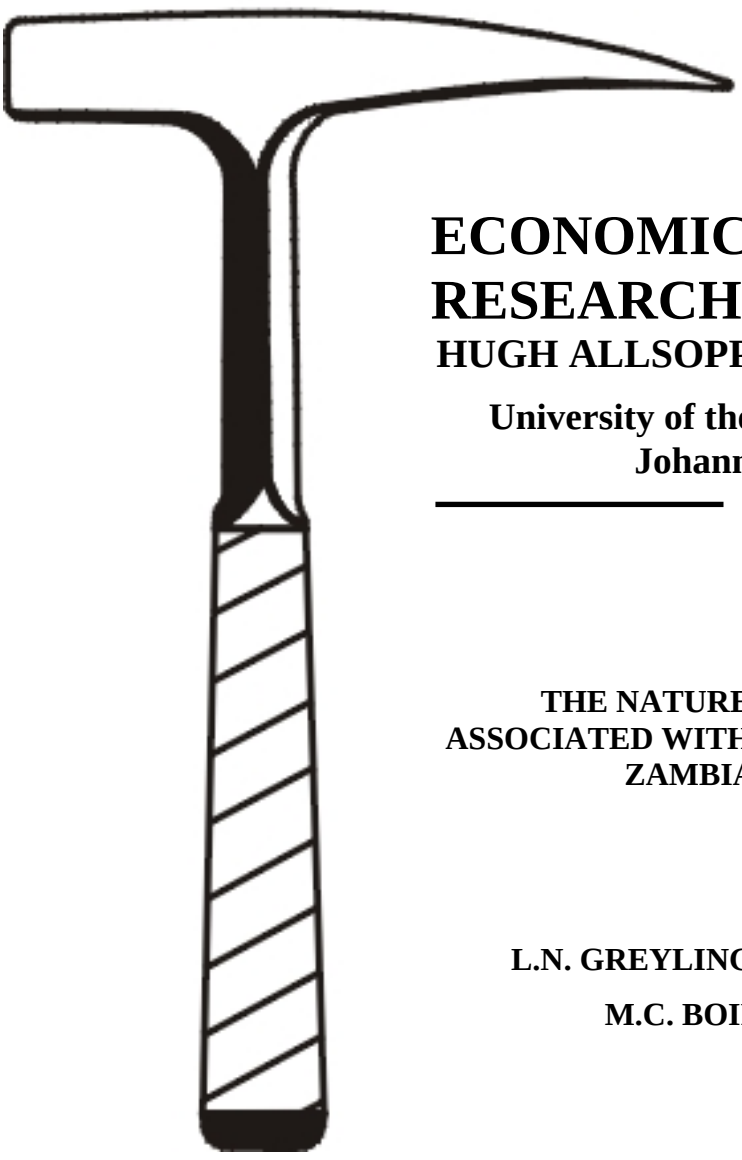

# ECONOMIC GEOLOGY RESEARCH INSTITUTE

## HUGH ALLSOPP LABORATORY

**University of the Witwatersrand**
**Johannesburg**

# THE NATURE OF BASINAL FLUIDS ASSOCIATED WITH THE CHAMBISHI DEPOSIT, ZAMBIAN COPPERBELT

**L.N. GREYLING, L.J. ROBB, S. MASTER**

**M.C. BOIRON, AND Y. YAO**

**INFORMATION CIRCULAR No. 385**

UNIVERSITY OF THE WITWATERSRAND
JOHANNESBURG

# THE NATURE OF BASINAL FLUIDS ASSOCIATED WITH THE CHAMBISHI DEPOSIT, ZAMBIAN COPPERBELT

**by**

**L.N. GREYLING[1]*, L.J. ROBB[1], S. MASTER[1], M.C. BOIRON[2] AND Y. YAO[1]**

*([1] Economic Geology Research Institute – Hugh Allsopp Laboratory, School of Geosciences, University of the Witwatersrand,Private Bag 3, 2050 WITS, Johannesburg, South Africa*
*[2] CREGU, Géologie et Gestion des Ressources Minérales et Energétiques, UMR 7566, Université Henri Poincaré, BP 23, Vandoeuvre-les-Nancy, 54506, France*

** corresponding author: greylin@science.pg.wits.ac.za (tel: +27 11 717 6580, fax: +27 11 717 6579)*

**ECONOMIC GEOLOGY RESEARCH INSTITUTE**
**INFORMATION CIRCULAR No. 385**

**November, 2004**

# THE NATURE OF BASINAL FLUIDS ASSOCIATED WITH THE CHAMBISHI DEPOSIT, ZAMBIAN COPPERBELT

## ABSTRACT

Fluid inclusions from a mineralised lateral secretion quartz vein-set in the Chambishi open pit in the Zambian Copperbelt represent fluids that immediately post-date stratiform copper mineralisation. Petrographic evidence indicates that this vein set predates deformation in the area. Fluid inclusion microthermometry and Raman spectroscopy of aqueous and aqueo-carbonic inclusions indicate the presence of an early saline $H_2O$-NaCl+$MgCl_2$±$CaCl_2$±$CO_2$ ±$CH_4$ ±$N_2$ fluid (11.9-23.1 wt.% $NaCl_{equiv}$) at homogenisation temperatures of 86-129°C. Later fluids occur in fluid inclusion planes and are linked to early metamorphism of the basin. These fluids are more varied in composition and are aqueous, aqueo-carbonic, and pure methane inclusions. Aqueous and aqueo-carbonic inclusions are $H_2O$-NaCl ±$CaCl_2$ ±$MgCl_2$ ±KCl ±$CO_2$, $N_2$, $CH_4$, $H_2S$ fluids, with two salinity end-members, namely, a high salinity (18-23 wt.% $NaCl_{equiv}$) - lower temperature (~130-160°C) fluid, and a lower salinity (~6 wt.% $NaCl_{equiv}$) - higher temperature (~140-210 °C) fluid. Later carbonic inclusion planes contain $CH_4$, with $N_2$ and $C_2H_6$. Later fluids are complex in composition, salinity, and homogenisation temperatures and are thought to be late-diagenetic on the one hand, and early (methane productive) metamorphic on the other. Pressure and temperature conditions in the environment immediately after stratiform copper mineralisation occurred were around 480-800 bar and 130-270 °C.

**_____oOo_____**

# THE NATURE OF BASINAL FLUIDS ASSOCIATED WITH THE CHAMBISHI DEPOSIT, ZAMBIAN COPPERBELT

## CONTENTS



**_____oOo_____**


**Published by the Economic Geology Research Institute**
**(incorporating the Hugh Allsopp Laboratory)**
**School of Geosciences**
**University of the Witwatersrand**
**1 Jan Smuts Avenue**
**Johannesburg**
**South Africa**
**http://www.wits.ac.za/geosciences/egri.htm**

**ISBN 0-9584855-2-6**

# THE NATURE OF BASINAL FLUIDS ASSOCIATED WITH THE CHAMBISHI DEPOSIT, ZAMBIAN COPPERBELT

## INTRODUCTION

The Neoproterozoic stratiform Cu-Co ores of the Central African Copperbelt are hosted mainly by the Roan Group at the base of the Katanga Supergroup. This metallogenic province is situated on the border between Zambia and the Democratic Republic of the Congo (DRC), and is preserved in the Lufulian Arc (Fig. 1). Theories on the origin of mineralisation of these sediment-hosted stratiform copper deposits have ranged from syngenetic (Garlick, 1961; Fleischer, 1984; Sweeney and Binda, 1994) to epigenetic (Jackson, 1932; McGowan *et al*., 2003). However, recent models of ore deposition favour either early- or late diagenesis (Robb, 2005). In addition, the presence of a variety of epigenetic ores such as the Cu-Au, U- (Cu-Co-Ni-Mo), and Zn-Pb-Cu-Ge-Ga deposits within the Katanga metallogenic province illustrates the scale and complexity of mineralisation styles. Therefore, regional metallogenesis is best viewed in a polygenetic framework. This paper describes the fluid inclusion character of quartz veins from the Chambishi deposit (Figs. 1, 2). This forms part of a regional fluid study aimed at deciphering and documenting the characteristics and evolution of early fluids (late diagenetic), possibly associated with mineralisation, and late fluids (trapped during regional metamorphism post-dating stratiform mineralisation).

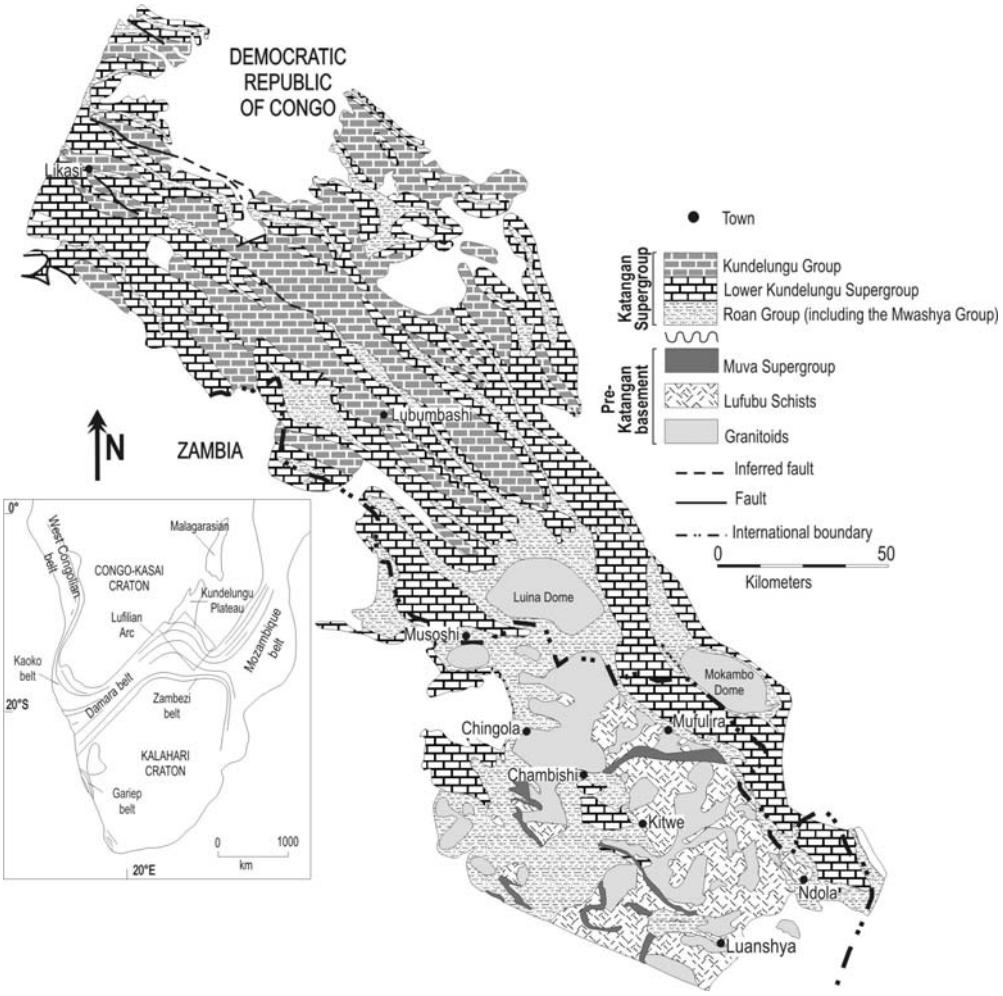


**Figure1:** *General geology of the Central African Copperbelt, showing the location of the Chambishi deposit in Zambia (modified from François, 1974 and Rainaud* et al.*, 2003).*

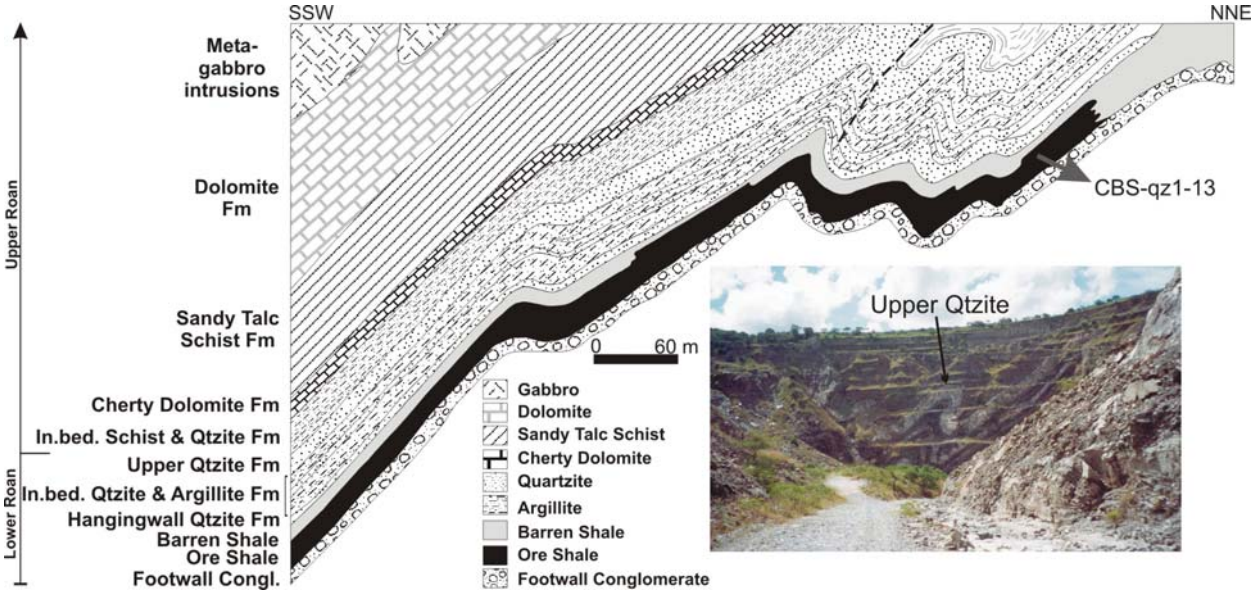


**Figure 2:** *Cross section of the Chambishi Main deposit (after Garlick, 1961), showing an asymmetrical fold in the now abandoned open pit. Regional thrusting occurred to the northeast as a result of compression during the Pan African Lufilian orogeny. The location of the samples for this study is indicated in the Ore Shale horizon.*

## GEOLOGICAL SETTING

The stratiform copper deposits of the Central African Copperbelt are hosted by the meta-sediments of the Neoproterozoic Katanga Supergroup (Fig. 1). The Katanga Supergroup unconformably overlies a basement comprised of an exposed Palaeoproterozoic calc-alkaline volcanic arc terrane (Rainaud *et al*., 1999), which in turn overlies a Mesoarchaean terrane (Rainaud *et al*., 2003). This basement is intruded by granitoids, which constrains the maximum age of Katangan sedimentation (Armstrong *et al*., 1999). The Katanga succession in Zambia is composed of the Roan, Mwashya, Nguba, and Kundelungu Groups, as specified by Wendorff (2003). Sedimentation of the Katanga occurred between 880 Ma (Armstrong *et al*., 1999) and 620 Ma (Cahen *et al*., 1984), with the onset of the Roan Group arenites, argillites, and shales deposited during rifting (Wendorff, 2003). According to Wendorff (2003), the Roan Group is overlain by the Mwashya Group, unconformably in the Kafue anticline region in Zambia, and non-conformably on the pre-Katanga basement in the DRC. Two tillites are present in the Nguba Group, which is comprised of marine siliciclastics and carbonate rocks. The base of the Nguba Group is indicated by the first tillite, the so-called Grand Conglomérat, which probably corresponds to the Sturtian glaciation (Robb *et al*., 2002; Robb, 2005).

The Katanga sediments were metamorphosed during the Lufilian orogenic event at *c*. 600-500 Ma (John *et al*., 2002) to greenschist facies in the Zambian Copperbelt, and to amphibolite facies in the Solwezi area to the west of the Copperbelt, with a general decrease in grade to the northeast, towards the DRC (Mendelsohn, 1961a). The Katanga metasediments are preserved in several structural basins (e.g., Konkola, Chambishi, Roan).

## REGIONAL STRATIFORM COPPER MINERALISATION

Mineralisation in Zambia and the DRC is mainly hosted in the lower Roan Group, but minor occurrences of mineralisation are also found in the basement and in the dolomites of the Nguba

Group. Ore minerals are mostly sulphides (including bornite, chalcocite, chalcopyrite, carrollite, and pyrite), and secondary oxides. Mineralisation in the lower Roan Group is hosted in two lithologies, namely, argillaceous shales and arenaceous quartzites and arkoses. Generally, the deposits of the Ore Shale (Fig. 2) are located along the west of the Kafue anticline (Fig. 1). The Ore Shale consists mostly of silty, micaceous (biotite or sericite ± muscovite), calcareous grains, with quartz, feldspar, carbonate, Cu-Fe sulphides, chlorite and organic carbon. The thickness varies from 5-20 m, and sulphides are generally disseminated through the Ore Shale, with concentrations along bedding planes (Mendelsohn, 1961b). The sericitic quartzite-hosted deposits are found along the eastern flank of the Kafue anticline in the Mufulira area (Fig. 1).

## PREVIOUS FLUID INCLUSION STUDIES: ZAMBIA AND THE DRC

Previous fluid inclusion studies in Zambia and the DRC include work by Pirmolin (1970), Sweeney (1987), Richards *et al*. (1988a), Speiser *et al*. (1995), and Kamona (1993). A summary of the main results is presented in Table 1, with the section below outlining the main findings of each of these studies.

- Pirmolin (1970) described fluid inclusions from an unmineralised cherty dolomite layer of the Mines Group of the Roan Group at Kamoto in the DRC, and concluded that the solutions in this area reached temperatures of ~200°C at salinities of ~40 wt. % $NaCl_{equiv}$ .
- Crosscutting quartz veins at the Konkola and Chambishi Cu-Co deposits were studied by Sweeney (1987). These veins had undergone at least one post-formational tectono-thermal event. Scanning electron microscopy of decrepitated inclusion cavities showed the presence of Na, Al, Si, S, U, K, Ca, Fe, Cu, and Co, and KCl, NaCl daughter minerals. Gas analyses of decrepitated inclusions revealed the presence of $CO_2$, $CH_4$, and $N_2$. It was concluded that the veins formed by lateral migration of fluids during late diagenetic dewatering.
- Richards *et al*. (1988a) indicated the presence of a sylvite-halite-saturated fluid in quartz-hematite-rutile veins hosted in the footwall sediments of the Musoshi copper deposit (DRC), where late hydrothermal veining caused extensive footwall- and Ore Shale- alteration. Fluid inclusions were found to consist of NaCl, KCl ± $CO_2$. This hydrothermal event postdates stratiform copper mineralisation and is linked to compressional deformation and metamorphism during the Lufilian orogeny. They estimated the maximum homogenisation pressure at 1.2 kbar, which is the typical pressure for decrepitation of 12-13µm size fluid inclusions in quartz (Leroy, 1979).
- Epigenetic iron-oxide-Cu-Au type mineralisation at the Kansanshi Copper Mine (Solwezi area, northwestern Zambia) was studied by Speiser *et al.* (1995) and Speiser (1994). Hydrothermal veining at Kansanshi is connected with alteration of the host rocks, and mineralised (Cu-Mo-Fe) veins have been dated at ~503-511 Ma (Re-Os and U-Pb of molybdenite and monazite) by Torrealday *et al.* (1999). Mineralisation at the Kansanshi Mine may also correspond to mineralisation at the Shinkwelobwe Mine (Cu-U), which is dated at 602 Ma (U/Pb, Cahen and Snelling, 1984). This style of mineralisation post-dated host-rock metamorphism.
- Kamona (1993) studied fluids from the epigenetic stratabound carbonate-hosted Pb-Zn Kabwe deposit, central Zambia. This epigenetic deposit is hosted by the Kabwe Dolomite Formation, where mineralising fluids were saline, ranging between 11-31 wt.% $NaCl_{equiv}$, and $T_h$ ranged between 257 and 305°C, corresponding to ore deposition at 320°C.
- Kampunzu *et al.* (1998) reported fluid inclusions from the epigenetic sediment-hosted Pb-Zn Kipushi deposit with high homogenisation temperatures (300°C) as temperatures of mineralising fluids. This style of mineralisation post-dates stratiform copper mineralisation.

**Table 1. Comparative results of previous fluid inclusion studies on Cu-Co and Pb-Zn deposits in the Central African Copperbelt**

| | **Pirmolin (1970)** | **Sweeney (1987)** | **Richards et al. (1988)** | **Kamona (1993)** | **Speiser et al. (1995)** | **Kampunzu et al., (1998)** |
|---|---|---|---|---|---|---|
| **Area** | Kamoto, DRC-Copperbelt | Konkola, Chambishi, Z-Copperbelt | Musoshi, DRC-Copperbelt | Kabwe, Central Zambia | Kansanshi, Solwezi, NW Zambia | Kipushi D.R.C. |
| **Lithology** | Mines Group, Roan | L. Roan Group | L. Roan Group | L. Kundelungu Group | ? | ? |
| **Minerals** | Cherty dolomite | Quartz veins | Quartz-hematite-uraninite veins | Dolomite | Quartz veins | ? |
| **Setting** | Epigenetic stratiform Cu | Late diagenetic stratiform Cu | Epigenetic U-Pb hydrothermal | Epigenetic Pb-Zn | Epigenetic Fe-ox-Cu-Au | epigenetic |
| **Composition** | ~40 wt.% NaClequiv. | $H_2O$, KCl, NaCl, $CO_2$, $CH_4$, $N_2$ | $H_2O$, KCl-NaCl-$CaCl_2$-$FeCl_3$-$CO_2$, 39 wt.% NaCl, 15 wt.% KCl | 11-31 wt.% NaClequiv. | $H_2O$, NaCl-$CaCl_2$-$CO_2$-($CH_4$) | ? |
| **P (kbar)** | ? | ? | <1.2 | 0.09 | 1.2 - 2.5 | ? |
| **Th (°C)** | ? | 120 | ~397<br>~275 | 257-305 | 230 - 310 | ca. 300 |

The work of Pirmolin (1970) and Sweeney (1987) is relevant to the present study. Their data indicate that fluids circulated early during the basin evolution, and were saline with moderate homogenisation temperatures. The present study, however, provides information on a vein set in a mineralised setting, where the tectonic and paragenetic relationships are better constrained. Accordingly, this study will add to existing knowledge of early tectonic fluids.

## CHAMBISHI COPPER DEPOSIT

Two deposits are identified in the Chambishi area, namely the Chambishi Main and the Chambishi West orebodies (Garlick, 1961; Garlick, 1976), where the Katanga metasediments unconformably overlie the 2050-1850 Ma basement comprising granitoids and the Lufubu schists (Master *et al.*, 2004; Rainaud *et al.*, 2004). The Katanga metasediments are preserved along the northern rim of the Chambishi-Nkana basin, striking east-west, and dipping south at about 60° (Garlick, 1961). The Ore Shale in this area consists of carbonaceous shale, siltstone, argillite, and interbedded dolomite (Fig. 2). Disseminated copper (± cobalt) sulphide mineralisation is present within the Ore Shale of the lower Roan Group (Fleischer, 1984). Zonation of chalcopyrite-bornite-chalcocite is present in the Ore Shale. The barren shale overlying the Ore Shale is mineralised with disseminated pyrite. Secondary malachite occurs as an oxidation product of primary sulphides.

Copper mineralisation in the Ore Shale was followed by the formation of bedding parallel quartz veins. Figure 3A illustrates a depleted halo surrounding a quartz vein where copper sulphides have been remobilized from the shale into the quartz vein. The mineralised sediments were subsequently metamorphosed and folded resulting in the development of an axial planar cleavage (Fig. 3B). This cleavage is refracted through the quartz vein (Fig. 3C), indicating a process of lateral secretion prior to metamorphism (see Fig. 3D).

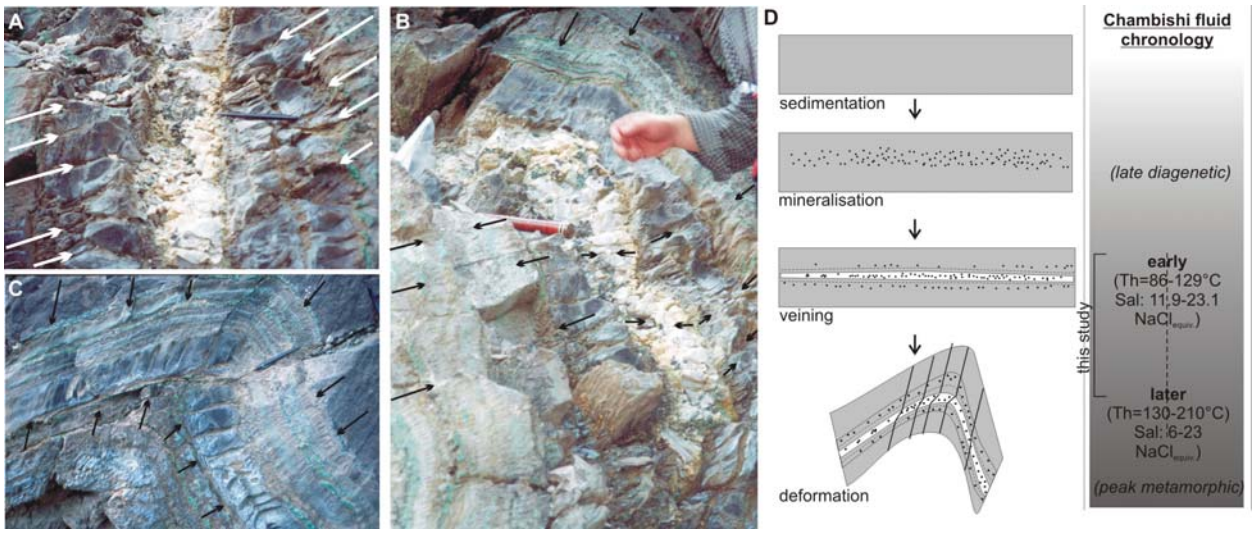


**Figure 3:** *Lateral secretion of primary copper mineralisation from the surrounding shale into a quartz vein, leaving a halo, depleted of mineralisation, surrounding the quartz vein in the Ore Shale horizon (A). The axial planar cleavage (B), produced during folding of the Ore Shale, is refracted by the intruding vein (C), which shows that the introduction of the vein preceded folding of the strata, but post-dated the stratiform mineralisation.*

## CHAMBISHI FLUID INCLUSIONS

### Sample selection

Samples were selected from the quartz vein hosted in the Ore Shale Formation illustrated in Figure 3. The early pre-orogenic tectonic setting of this particular vein is indicated by the axial planar cleavage, which is refracted from the shale through the quartz vein.

### Petrography

Certain minerals host fluid inclusions, which become trapped either during, or subsequent to, crystal growth (Goldstein and Reynolds, 1994). The relationship between individual inclusions, and amongst inclusions and growth zones, indicates the relative timing of entrapment. Based on petrographic observations, fluid inclusions and fluid inclusion assemblages may be identified as primary, secondary, or pseudo-secondary (Roedder, 1984; Goldstein and Reynolds, 1994). Assuming that no leaking or resetting has occurred during metamorphism in the Chambishi basin, primary inclusions found in this setting are interpreted as representative of pre-metamorphic fluids. Conversely, pseudo-secondary and secondary inclusions will be distinctive of fluids present during (and to some extent after) metamorphism.

In this study double-polished quartz wafers showed no growth zonation during optical microscopy or cathodoluminescence. However, a few small (<10µm), isolated inclusions are interpreted to be of primary origin based on their isolated distribution among secondary fluid inclusion planes (FIP's) (Fig. 4 D, E, H, I). These inclusions are interpreted to be representative of post-mineralising, pre-metamorphic fluids. Secondary fluid inclusions form when fluid is trapped during healing of microcracks, shear planes, or along twin planes or cleavage directions after crystal formation (Goldstein and Reynolds, 1994). The majority of inclusions documented here are interpreted as secondary. Therefore, inclusions in trails and fluid inclusion planes have trapped later fluids that also post-date mineralisation, but are coeval with deformation (Fig. 4 A-C, G, J-L). This study reports the characteristics of fluids trapped subsequent to mineralisation, and coeval with deformation of the Chambishi basin.

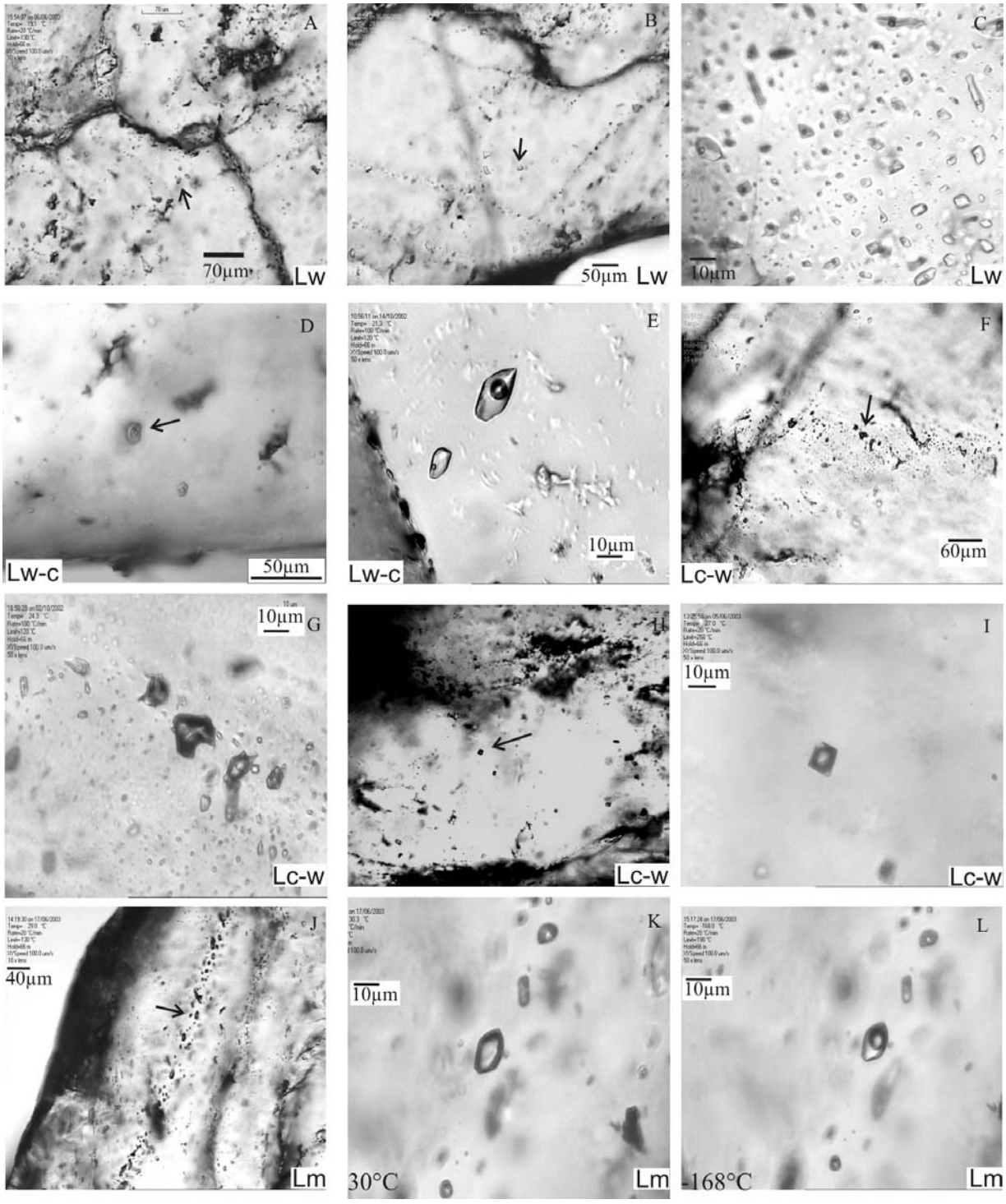


**Figure 4:** *Photomicrographs of typical fluid inclusion types in quartz. All images taken at room temperature, unless otherwise stated on the figure.*

*A: Isolated aqueous fluid inclusions (sample CBS-qz8A[1]9)*
*B: Isolated aqueous fluid inclusions (sample CBS-qz8A[1]2)*
*C: Secondary fluid inclusion planes (FIP's) of aqueous inclusions (CBS-qz3A[4])*
*D: Isolated aqueo-carbonic inclusions (CBS-qz8A[1]3)*
*E: FIP's aqueo-carbonic inclusion (CBS-qz3By[4]1)*
*F-G: Secondary aqueo-carbonic trail fluid inclusions trail(CBS-qz6A[2])*
*H-I: Isolated aqueo-carbonic inclusion with negative crystal shape (CBS-qz3A[6]10)*
*J-L: Secondary methane inclusions preserved in fluid inclusion planes (CBS-qz7BA[1]4).*

## Methodology

Double polished wafers of ~200 µm thickness were used for the petrographic and microthermometric study. Microthermometry was performed on a Linkam TH600 stage connected to an Olympus Vanox binocular microscope. The accuracy of the measurements was of ± 0.1°C at low temperatures and ± 2°C at high temperatures. Inclusions were cooled to -170°C and phase transitions were measured during heating. Estimates of the volumes of volatile phases at room temperature was undertaken using the volumetric estimation chart of Roedder (1972). The gaseous molar fractions were determined using a Raman Labram Jobin-Yvon microspectrometer, with an ionised Ar laser (wavelength 514.5 nm) as excitation source. The laser was focused on the sample with an 80x objective lens.

Fluid inclusion types are defined according to the nomenclature used by Boiron *et al*. (1992). Inclusions are classified based on their final homogenisation ($T_ht$) behaviour (see Table 2), L: into the liquid phase, V: into the vapour phase, and presence of dominant aqueous (w) or carbonic (c) species (see Table 2 for explanation of abbreviations). Salinities for the aqueous inclusions were calculated from $T_m(ice)$ using the equations in Bodnar and Vityk (1994). Salinities for aqueo-carbonic inclusions were calculated using degree of fill, $T_h(CO_2)$ and $T_m(clath)$ by using the equation of state in Bodnar (1983) and Brown and Lamb (1986, 1989) in the Linkam Scientific PVTX Software Modelling programme for Fluid Inclusions, V 2.1. Bulk densities of FIP's were calculated using the computer programme *Bulk*, version 01/03 (Bakker, 2003), and isochors were calculated and plotted using *Isochor* version 13/03/96 (Bakker, 1997) and *Isoc* version 01/03 (Bakker, 2003) utilizing the Bowers and Helgeson (1983) and Zhang and Frantz (1987) equations of state.

**Table 2. Explanation of abbreviations used in microthermometric interpretations (from Goldstein and Reynolds, 1994; Boiron *et al*., 1992; Diamond, 2003)**

| | |
|---|---|
| $T_ht$ | temperature of final homogenisation |
| L | homogenisation to the liquid phase |
| $T_e$ | eutectic temperature |
| $T_m(hh)$ | melting of hydrohalite |
| $T_m(ice)$ | final ice melting |
| $T_m(CO_2)$ | final melting of $CO_2$ |
| $T_m(cla)$ | final melting of clathrate |
| $T_h(CO_2)$ | homogenization of the carbonic phase |
| c | gaseous phases including $CO_2$, $N_2$, $CH_4$, $H_2S$ |
| m | methane dominantly present |
| FIPs | fluid inclusion planes |

## Fluid inclusion types

Fluid inclusions were found preserved as isolated occurrences, in trails, and in planes. The types were defined using the abovementioned nomenclature of Boiron *et al*. (1992). Selected representative data is presented in Table 3. The following types were identified:

**Table 3. Results of microthermometry and Raman spectroscopy for all primary and secondary fluid inclusion types**

| | | | | Microthermometry | | | | | | | | | Raman (mol%) | | | | | Bulk composition | | | | | | |
|---|---|---|---|---|---|---|---|---|---|---|---|---|---|---|---|---|---|---|---|---|---|---|---|---|
| Sample | FI | %vap | Type | Te | $Tm_{hh}$ | $Tm_{ice}$ | $Th_{tot}$ | Mode | $TmCO_2$ | $ThCO_2$ | Mode | $Tm_{cla}$ | $CO_2$ | $N_2$ | $H_2S$ | $CH_4$ | $C_2H_6$ | $H_2O$ | $CO_2$ | $N_2$ | $CH_4$ | NaCl | ρ (g/cc) | $NaCl_{eq.}$ |
| ***isolated*** | | | | | | | | | | | | | | | | | | | | | | | | |
| ***aqueous*** | | | | | | | | | | | | | | | | | | | | | | | | |
| Cbsqz8A | (1)1 | 10 | Lw | -35 | - | -21.1 | dec | | - | - | - | - | - | - | - | - | - | | | | | | | 23.1 |
| Cbsqz8A | (1)2 | 10 | Lw | -47 | - | -21.1 | 129 | L | - | - | - | - | - | - | - | - | - | | | | | | | 23.1 |
| Cbsqz8A | (1)5 | 20 | Lw | <-25 | -21 | -12.3 | - | - | - | - | - | - | - | - | - | - | - | | | | | | | 16.2 |
| Cbsqz8A | (1)6 | 10 | Lw | ~-50 | ~-21 | -9.5 | 110 | L | - | - | - | - | - | - | - | - | - | | | | | | | 13.4 |
| Cbsqz8A | (1)7 | 8 | Lw | -50 | ~-19 | -9.5 | 109 | L | - | - | - | - | - | - | - | - | - | | | | | | | 13.4 |
| Cbsqz8A | (1)8 | 10 | Lw | -50 | ~-19 | -9.5 | 107 | L | - | - | - | - | - | - | - | - | - | | | | | | | 13.4 |
| Cbsqz8A | (1)9 | 10 | Lw | -45 | ~-22 | -13.6 | 126 | L | - | - | - | - | - | - | - | - | - | | | | | | | 17.4 |
| Cbsqz8A | (1)10 | 10 | Lw | -45 | ~-22 | -13.6 | 129 | L | - | - | - | - | - | - | - | - | - | | | | | | | 17.4 |
| Cbsqz8A | (1)11 | 10 | Lw | -45 | ~-22 | - | 86 | L | - | - | - | - | - | - | - | - | - | | | | | | | |
| Cbsqz8A | (2)1 | 10 | Lw | ~-40 | -22.4 | -12.3 | - | | - | - | - | - | - | - | - | - | - | | | | | | | 16.2 |
| ***aqueo-carbonic*** | | | | | | | | | | | | | | | | | | | | | | | | |
| Cbsqz3A | (6)2 | 10 | Lw-c | -37 | -20.8 | - | | | | | - | 2.0 | 98.5 | ≤1 | | 0.6 | | 98.2 | 1.8 | | | | 0.90 | |
| Cbsqz3A | (6)10 | 60 | Lc-w | - | - | | - | - | -56.8 | 22.8 | L | 2 | >98.5 | 1 | | ≤0.2 | | 62.1 | 33.9 | 0.5 | | 3.5 | 0.86 | 13.2 |
| Cbsqz3A | (6)11 | 20 | Lw-c-s | - | - | - | - | - | -57.9 | 23.9 | L | 2 | 99 | ≤1 | | | | 85.4 | 9.7 | 0.1 | | 4.8 | 0.99 | |
| Cbsqz3A | (6)12 | 20 | Lw-c | - | - | - | - | - | -57.9 | 26.9 | L | 2.2 | >99.5 | ≤0.2 | ≤0.2 | | | 85.7 | 9.6 | 0.03 | | 4.7 | 0.98 | 12.9 |
| Cbsqz8A | (1)3 | 25 | Lw-c | - | - | - | >150 | L | -57.0 | 11.8 | L | 3.0 | 98 | ≤0.5 | | 2 | | 82.4 | 13 | 0.2 | | 4.4 | 0.99 | 11.9 |
| Cbsqz8A | (1)4 | 25 | Lw-c | - | - | - | >150 | L | - | 15.0 | L | 3.0 | | | | | | | | | | | | 11.9 |
| ***trails and fluid inclusion planes*** | | | | | | | | | | | | | | | | | | | | | | | | |
| ***aqueous*** | | | | | | | | | | | | | | | | | | | | | | | | |
| Cbsqz3A | (2)1 | 10 | Lw | -55 | -22.3 | -19.0 | 143 | L | - | - | - | - | - | - | - | - | - | | | | | | | 21.7 |
| Cbsqz3A | (2)2 | 10 | Lw | -51 | -22.1 | -18.6 | 148 | L | - | - | - | - | - | - | - | - | - | | | | | | | 21.4 |
| Cbsqz3A | (2)3 | 10 | Lw | -51 | -22.1 | -18.6 | 140 | L | - | - | - | - | - | - | - | - | - | | | | | | | 21.4 |
| Cbsqz3A | (2)4 | 10 | Lw | -53 | -22.6 | -14.6 | 150 | L | - | - | - | - | - | - | - | - | - | | | | | | | 18.3 |
| Cbsqz3A | (2)5 | 10 | Lw | -45 | - | -15.4 | 150 | L | - | - | - | - | - | - | - | - | - | | | | | | | 19.0 |
| Cbsqz3A | (4)1 | 10 | Lw | -54 | -22.9 | -20.8 | 154 | L | - | - | - | - | - | - | - | - | - | | | | | | | 22.9 |
| Cbsqz3A | (4)3 | 10 | Lw | -54 | -22.9 | -21.2 | 145 | L | - | - | - | - | - | - | - | - | - | | | | | | | 23.2 |
| Cbsqz3A | (4)4 | 10 | Lw | -54 | -23 | -21.2 | 154 | L | - | - | - | - | - | - | - | - | - | | | | | | | 23.2 |
| Cbsqz3A | (4)5 | 10 | Lw | -55 | -23.1 | -21.2 | 156 | L | - | - | - | - | - | - | - | - | - | | | | | | | 23.2 |
| Cbsqz3A | (4)9 | 10 | Lw | -53 | -22.5 | -21.2 | 155 | L | - | - | - | - | - | - | - | - | - | | | | | | | 23.2 |
| Cbsqz3A | (4)10 | 10 | Lw | -53 | -22.9 | -21.2 | 154 | L | - | - | - | - | - | - | - | - | - | | | | | | | 23.2 |
| Cbsqz3A | (6)0.1 | 10 | Lw | -52 | - | -18.9 | 131 | L | | | - | | - | - | - | - | - | | | | | | | 21.6 |
| Cbsqz3A | (6)1 | 10 | Lw | -39 | - | -3.2 | | | - | - | - | - | - | - | - | - | - | | | | | | | 5.3 |
| Cbsqz3A | (6)3 | 10 | Lw | -50 | -22.3 | -18.8 | | | | | - | | - | - | - | - | - | | | | | | | 21.5 |
| Cbsqz3A | (6)4 | 10 | Lw | -53 | -22.6 | -17.3 | | | - | - | - | - | - | - | - | - | - | | | | | | | 20.4 |
| Cbsqz3A | (6)5 | 10 | Lw | -45 | -22.6 | -17.5 | | | - | - | - | - | - | - | - | - | - | | | | | | | 20.6 |
| Cbsqz3A | (6)6 | 10 | Lw | -54 | -22.3 | -18.2 | | | - | - | - | - | - | - | - | - | - | | | | | | | 21.1 |
| Cbsqz3A | (6)7 | 10 | Lw | -47 | | -17.5 | | | - | - | - | - | - | - | - | - | - | | | | | | | 20.6 |
| Cbsqz3A | (6)8 | 10 | Lw | -55 | -21.8 | -14.5 | 140 | L | - | - | - | - | - | - | - | - | - | | | | | | | 18.2 |
| Cbsqz3Bx | (1)1 | 10 | Lw | -25 | - | -1.6 | - | - | - | - | - | - | - | - | - | - | - | | | | | | | 2.7 |
| Cbsqz3Bx | (1)2 | 10 | Lw | -23 | - | -1.7 | - | - | - | - | - | - | - | - | - | - | - | | | | | | | 2.9 |
| Cbsqz6A | (3)1 | 10 | Lw | ~-41 | - | -3.0 | 142 | L | - | - | - | - | - | - | - | - | - | | | | | | | 5.0 |
| Cbsqz6A | (3)2 | 25 | Lw | ~-26 | - | -4.0 | 192 | L | - | - | - | ~11 | - | - | - | - | - | | | | | | | 6.4 |
| Cbsqz6A | (3)3 | 15 | Lw | ~-29 | - | -3.9 | 208 | L | - | - | - | - | - | - | - | - | - | | | | | | | 6.3 |
| Cbsqz6A | (3)4 | 20 | Lw | - | - | -4.0 | 189 | L | - | - | - | ~8 | - | - | - | - | - | | | | | | | 6.4 |
| Cbsqz6A | (3)5 | 35 | Lw | ~-47 | - | -4.8 | 160 | L | - | - | - | - | - | - | - | - | - | | | | | | | 7.6 |
| Cbsqz6A | (3)6 | 25 | Lw | - | - | -4.0 | 178 | L | - | - | - | - | - | - | - | - | - | | | | | | | 6.4 |
| Cbsqz6A | (3)7 | 20 | Lw | | | | | | | | | | - | - | - | - | - | | | | | | | |
| Cbsqz6A | (3)8 | 20 | Lw | | | | | | | | | | - | - | - | - | - | | | | | | | |
| Cbsqz6A | (3)9 | 20 | Lw | ~-40 | - | -4.1 | 179 | L | - | - | - | - | - | - | - | - | - | | | | | | | 6.6 |
| Cbsqz6A | (3)10 | 20 | Lw | ~-39 | - | -4.1 | 177 | L | - | - | - | - | - | - | - | - | - | | | | | | | 6.6 |
| ***aqueo-carbonic*** | | | | | | | | | | | | | | | | | | | | | | | | |
| Cbsqz3A | (4)2 | 10 | Lw-c | -56 | -22.9 | -21.2 | 149 | L | -57.9 | | - | | | | | | | | | | | | | |
| Cbsqz3By | (4)1 | 20 | Lw-c | ~-32 | - | - | 245 | dec | -57.2 | 29.4 | L | 7.5 | 98.2 | 1.5 | ≤0.5 | <0.1 | | | | | | | | 4.8 |
| Cbsqz3By | (4)2 | 10 | Lw-c | - | - | -8.0 | 229 | L | -57.2 | 30.0 | L | 5 | 99.5 | <0.5 | ≤0.2 | | | | | | | | | 9.0 |
| Cbsqz3By | (4)3 | 20 | Lw-c | -35 | | -9.6 | 229 | L | -57.1 | 30.8 | L | 8.2 | | | | | | | | | | | | 3.6 |
| Cbsqz3By | (4)4 | 15 | Lw-c | - | - | - | 196 | L | - | 30.8 | L | - | | | | | | | | | | | | |
| Cbsqz3By | (4)5 | 40 | Lw-c | - | - | - | >300 | L | -56.9 | 30.8 | V | - | | | | | | | | | | | | |
| Cbsqz3By | (4)6 | 70 | Lc-w | - | - | - | >300 | V | -58.0 | 26.6 | L | - | 98.3 | 1.2 | ≤0.5 | | | | | | | | | |
| Cbsqz3By | (4)7 | 20 | Lw-c | - | - | - | - | - | -58.0 | 30.8 | L | - | 98.2 | 1.3 | ≤0.5 | <0.1 | | | | | | | | |
| Cbsqz3By | (4)8 | 20 | Lw-c | - | - | - | dec | - | - | - | - | - | | | | | | | | | | | | |
| Cbsqz3By | (4)9 | 50 | Lw-c | - | - | -10.0 | >300 | L | - | 28.3 | V | - | >99.8 | | ≤0.2 | | | | | | | | | |
| Cbsqz3By | (4)10 | 10 | Lw-c | - | - | -9.0 | 189 | L | - | 27.9 | L | ~5 | | | | | | | | | | | | 9.0 |
| CHM7BA | (1)1 | 10 | Lw-c | -51 | | -14.4 | | | | 27.5 | L | 2.6 | 98.0 | 2.0 | | 0.0 | | 89.9 | 4.7 | 0.1 | - | 5.3 | 1.00 | 12.5 |
| CHM7BA | (1)3 | 30 | Lw-c | ~-42 | ~-23.8 | -21.0 | | | -58.7 | 16.6 | L | 3.1 | 91.7 | 6.0 | | 2.3 | | 82.3 | 12.1 | 0.7 | 0.2 | 4.7 | 0.92 | 11.8 |
| CHM7BA | (1)4 | 30 | Lw-c | ~-48 | - | -23.8 | dec | | -56.9 | 19.6 | L | -0.4 | 98 | 1.7 | | 0.3 | | | | | | | | 16.0 |
| CHM7BA | (1)5 | 10 | Lw-c | - | - | - | 179 | L | | | | 1.1 | | | | | | | | | | | | |
| CHM7BA | (1)6 | 10 | Lw-c | -44 | ~-23 | -15.4 | 221 | L | | | | 1.7 | | | | | | | | | | | | |
| CHM7BA | (1)7 | 10 | Lw-(c) | ~-40 | - | -14.8 | 144 | L | | | | | | | | | | | | | | | | |
| CHM7BA | (1)8 | 10 | Lw-(c) | -39 | - | -15.7 | 150 | L | | | | | | | | | | | | | | | | |
| CHM7BA | (1)9 | 10 | Lw-(c) | ~-41 | ~-20 | -15.7 | | | | | | | 32 | 47.5 | | 6.5 | | | | | | | | |
| CHM7BA | (1)10 | 10 | Lw-c | -46 | ~-21 | -14.1 | 128 | L | | | | | | | | | | | | | | | | |
| CHM7BA | (1)11 | 15 | Lw-(c) | -44 | ~-22 | -12.8 | 211 | L | | | | -2.2 | 37 | 55.5 | | 7.5 | | | | | | | | |
| CHM7BA | (1)12 | 10 | Lw-(c) | -39 | ~-21 | -15.7 | 214 | L | | | | | | | | | | | | | | | | |
| CHM7BA | (1)13 | 8 | Lw-(c) | -42 | ~-21 | -15.4 | 205 | L | | | | | | | | | | | | | | | | |
| CHM7BA | (1)14 | 10 | Lw-(c) | -46 | ~-21 | -15.7 | | | | | | | | | | | | | | | | | | |
| CHM7BA | (1)15 | 10 | Lw-(c) | -42 | ~-21 | -15.5 | | | | | | | | | | | | | | | | | | |
| CHM7BA | (1)16 | 10 | Lw-(c) | - | - | -15.2 | | | | | | | | | | | | | | | | | | |
| CHM7BA | (1)17 | 10 | Lw-(c) | -41.3 | ~-21 | -15.7 | | | | | | | | | | | | | | | | | | |

| | | | | | | | | | | | | | | | | | | | | | | | |
|---|---|---|---|---|---|---|---|---|---|---|---|---|---|---|---|---|---|---|---|---|---|---|---|
| CHM7BA | (1)18 | 10 | Lw-(c) | -39 | - | -15.2 | | | | | | | | | | | | | | | | | |
| CHM7BA | (1)19 | 10 | Lw-(c) | ~-39 | - | -13.0 | | | | | | 5 | | | | | | | | | | | |
| CHM7BA | (1)20 | 10 | Lw-(c) | -35 | - | -11.8 | | | | | | 5 | | | | | | | | | | | |
| Cbsqz6A | (2)2 | 90 | Lc-w | - | - | - | - | - | -57.3 | 21.0 | L | -2 | 98.2 | 1.3 | ≤0.5 | | | 22.5 | 74.5 | 1.3 | | 1.7 | 0.77 | 17.7 |
| Cbsqz6A | (2)3 | 65 | Lc-w | - | - | - | - | - | -57.1 | 27.5 | L | - | | | | | | | | | | | | |
| Cbsqz6A | (2)4 | 85 | Lc-w | - | - | - | - | - | -57.5 | 27.5 | L | - | 98.2 | 1.3 | ≤0.5 | | | 92.8 | 7.1 | 0.1 | | - | 0.92 | |
| Cbsqz6A | (2)5 | 75 | Lc-w | - | - | - | - | - | -57.2 | 29.5 | L | 6.5 | 98.2 | 1.3 | ≤0.5 | | | 57.5 | 40 | 0.6 | | 1.9 | 0.62 | 6.6 |
| Cbsqz6A | (2)6 | 75 | Lc-w | - | - | - | - | - | -57.5 | 30.2 | L | 7.0 | 98.5 | 1.1 | ≤0.5 | | | | | | | | | 5.8 |
| Cbsqz6A | (2)7 | 90 | Lc-w | - | - | - | - | - | -57.2 | 27.8 | L | 7.4 | 98.6 | 1.3 | <0.1 | | | 27.2 | 71.1 | 0.9 | | 0.8 | 0.67 | 5.1 |
| Cbsqz6A | (2)8 | 70 | Lc-w | - | - | - | - | - | -57.3 | 26.8 | L | 6.5 | 98.3 | 1.2 | ≤0.5 | | | 56.3 | 41.4 | 0.5 | | 1.8 | 0.77 | 6.6 |
| Cbsqz6A | (2)9 | 80 | Lc-w | - | - | - | - | - | - | 27.9 | L | - | | | | | | | | | | | | |
| Cbsqz7BA | (1)2 | 15 | Lw-c-s | ~-50 | | -16.2 | | | -23.7 | | L | 5.9 | 59 | 5.5 | | 35.5 | <0.1 | 90.9 | 2.9 | 0.1 | 0.7 | 5.4 | 0.94 | 19.6 |
| ***carbonic-methane*** | | | | | | | | | | | | | | | | | | | | | | | | |
| Cbsqz7BA | (1)1 | 100 | Lm | - | - | - | - | - | - | -88.1 | L | - | nd | 6.5 | | 93 | 0.5 | | | | | | | |
| Cbsqz7BA | (1) 2 | 100 | Lm | - | - | - | - | - | - | -87.8 | L | - | - | - | - | - | - | | | | | | | |
| Cbsqz7BA | (1) 3 | 100 | Lm | - | - | - | - | - | - | -87.8 | L | - | - | - | - | - | - | | | | | | | |
| Cbsqz7BA | (1) 4 | 100 | Lm | - | - | - | - | - | - | -87.7 | L | - | - | - | - | - | - | | | | | | | |
| Cbsqz7BA | (1) 5 | 100 | Lm | - | - | - | - | - | - | -88.0 | L | - | - | - | - | - | - | | | | | | | |
| Cbsqz7BA | (1) 6 | 100 | Lm | - | - | - | - | - | - | -87.9 | L | - | - | - | - | - | - | | | | | | | |
| Cbsqz7BA | (1)7 | 100 | Lm | - | - | - | - | - | - | - | - | - | nd | 6.5 | | 93 | 0.5 | | | | | | | |
| Cbsqz7BA | (1)8 | 100 | Lm | - | - | - | - | - | - | -87.9 | L | - | nd | 7 | | 92 | 1 | | | | | | | |
| Cbsqz7BA | (1) 9 | 100 | Lm | - | - | - | - | - | - | -87.9 | L | - | - | - | - | - | - | | | | | | | |
| Cbsqz7BA | (1) 10 | 100 | Lm | - | - | - | - | - | - | -87.9 | L | - | - | - | - | - | - | | | | | | | |
| Cbsqz7BA | (1) 11 | 100 | Lm | - | - | - | - | - | - | -87.9 | L | - | - | - | - | - | - | | | | | | | |
| Cbsqz7BA | (1) 12 | 100 | Lm | - | - | - | - | - | - | -87.7 | L | - | - | - | - | - | - | | | | | | | |
| Cbsqz7BA | (1) 13 | 100 | Lm | - | - | - | - | - | - | -87.7 | L | - | - | - | - | - | - | | | | | | | |
| Cbsqz7BA | (1) 14 | 100 | Lm | - | - | - | - | - | - | -88.2 | L | - | - | - | - | - | - | | | | | | | |
| Cbsqz7BA | (1) 15 | 100 | Lm | - | - | - | - | - | - | -88.2 | L | - | - | - | - | - | - | | | | | | | |
| Cbsqz7BA | (1) 16 | 100 | Lm | - | - | - | - | - | - | -88.4 | L | - | - | - | - | - | - | | | | | | | |
| Cbsqz7BA | (1) 17 | 100 | Lm | - | - | - | - | - | - | -88.6 | L | - | - | - | - | - | - | | | | | | | |
| Cbsqz7BA | (1) 18 | 100 | Lm | - | - | - | - | - | - | -88.5 | L | - | - | - | - | - | - | | | | | | | |
| Cbsqz7BA | (1) 19 | 100 | Lm | - | - | - | - | - | - | -88.5 | L | - | - | - | - | - | - | | | | | | | |
| Cbsqz7BA | (1) 20 | 100 | Lm | - | - | - | - | - | - | -87.7 | L | - | - | - | - | - | - | | | | | | | |
| Cbsqz7BA | (1) 21 | 100 | Lm | - | - | - | - | - | - | -87.7 | L | - | - | - | - | - | - | | | | | | | |
| Cbsqz7BA | (1) 22 | 100 | Lm | - | - | - | - | - | - | -88.1 | L | - | - | - | - | - | - | | | | | | | |
| Cbsqz7BA | (1) 23 | 100 | Lm | - | - | - | - | - | - | -88.2 | L | - | - | - | - | - | - | | | | | | | |
| Cbsqz7BA | (1) 24 | 100 | Lm | - | - | - | - | - | - | -87.8 | L | - | - | - | - | - | - | | | | | | | |
| Cbsqz7BA | (1) 25 | 100 | Lm | - | - | - | - | - | - | -88.3 | L | - | - | - | - | - | - | | | | | | | |
| Cbsqz7BA | (1) 26 | 100 | Lm | - | - | - | - | - | - | -88.1 | L | - | - | - | - | - | - | | | | | | | |
| Cbsqz7BA | (1) 27 | 100 | Lm | - | - | - | - | - | - | -88.2 | L | - | - | - | - | - | - | | | | | | | |
| Cbsqz7BA | (1)28 | 100 | Lm | - | - | - | - | - | - | - | - | - | nd | 7 | | 92.5 | 0.5 | | | | | | | |
| Cbsqz7BA | (1) 29 | 100 | Lm | - | - | - | - | - | - | -88.2 | L | - | - | - | - | - | - | | | | | | | |
| Cbsqz7BA | (1) 30 | 100 | Lm | - | - | - | - | - | - | -88.2 | L | - | - | - | - | - | - | | | | | | | |
| Cbsqz7BA | (1) 31 | 100 | Lm | - | - | - | - | - | - | -88.1 | L | - | - | - | - | - | - | | | | | | | |
| Cbsqz7BA | (1) 32 | 100 | Lm | - | - | - | - | - | - | -88.0 | L | - | - | - | - | - | - | | | | | | | |
| Cbsqz7BA | (1) 33 | 100 | Lm | - | - | - | - | - | - | -88.4 | L | - | - | - | - | - | - | | | | | | | |
| Cbsqz7BA | (1) 34 | 100 | Lm | - | - | - | - | - | - | -88.1 | L | - | - | - | - | - | - | | | | | | | |
| Cbsqz7BA | (1) 35 | 100 | Lm | - | - | - | - | - | - | -88.1 | L | - | - | - | - | - | - | | | | | | | |
| Cbsqz7BA | (1) 36 | 100 | Lm | - | - | - | - | - | - | -88.7 | L | - | - | - | - | - | - | | | | | | | |
| Cbsqz7BA | (1) 37 | 100 | Lm | - | - | - | - | - | - | -87.9 | L | - | - | - | - | - | - | | | | | | | |
| Cbsqz7BA | (1) 38 | 100 | Lm | - | - | - | - | - | - | -88.1 | L | - | - | - | - | - | - | | | | | | | |
| Cbsqz7BA | (1) 39 | 100 | Lm | - | - | - | - | - | - | -88.2 | L | - | - | - | - | - | - | | | | | | | |
| Cbsqz7BA | (1)40 | 100 | Lm | - | - | - | - | - | - | -88.3 | L | - | - | - | - | - | - | | | | | | | |
| Cbsqz7BA | (1)41 | 100 | Lm | - | - | - | - | - | - | -86.5 | L | - | - | - | - | - | - | | | | | | | |

***(1) aqueous inclusions***

Aqueous fluid inclusions are found as both isolated inclusions (Fig. 4A-B) and secondary planes (Fig. 4C). Initial melting of isolated inclusions at between -50 and -35 °C is interpreted to be eutectic melting. Eutectic melting temperatures of isolated inclusions indicate the presence of $H_2O$-NaCl+$MgCl_2$±$CaCl_2$ (Goldstein and Reynolds, 1994). Isolated inclusions range in size between 12-30µm diameter, with 8-20% vapour. Final ice melting temperatures ($T_m$*(ice)*) for isolated inclusions range from -9.5°C to -21.1°C (Fig. 5A), corresponding to salinities of between 13.4 and 23.1 wt.% $NaCl_{equiv}$. Final homogenisation ($T_h$*t*) was to the liquid phase ranging from 86 to 129°C (Fig. 5B).

Aqueous fluid inclusions in trails and in planes contain 10-35% vapour. Initial melting of aqueous phases, interpreted as eutectic melting ($T_e$), occurred between -55 and -23 °C, which corresponds to a composition of $H_2O$-NaCl±$CaCl_2$±$MgCl_2$±KCl (Goldstein and Reynolds, 1994). $T_m$*(ice)* for FIP's ranges from -1.6 to -21.2 °C (Fig. 5A), indicating salinities between 2.7 and 23.2 wt.% $NaCl_{equiv}$ Total homogenisation ($T_h$*t*) for FIP's was always to the liquid phase, between 131 and 208 °C (Fig. 5B).

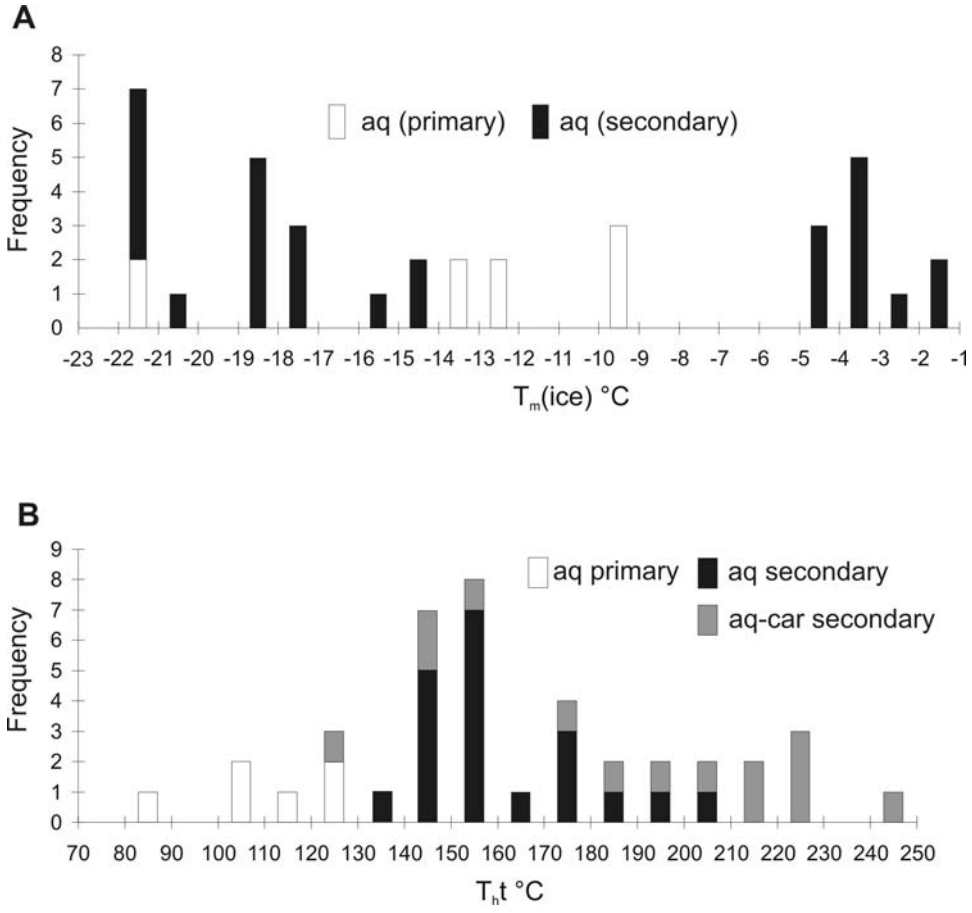


**Figure 5:** *A: Histogram showing the distribution of the final ice melting temperatures ($T_m$ice) of aqueous isolated (primary) and trail (secondary) inclusions. B: Histogram showing the final homogenisation temperature ($T_h$t in °C) distribution of all aqueous and aqueous carbonic inclusions.*

***(2) aqueo-carbonic inclusions***

Several inclusions consist of mixed aqueous and non-aqueous phases. The non-aqueous components (carbonic) refer to $CO_2$, $CH_4$, $N_2$, $C_2H_6$ and $H_2S$. Isolated aqueo-carbonic inclusions (Fig. 4 D, H-I) range in size between 8-20µm, with between 10-60% vapour. This inclusion type also occurs as secondary trails (Fig. 4 E-G), with vapour phases ranging between 8 and 90 vol%.

Melting of isolated carbonic phases ($T_m(CO_2)$) are between -56.8 and -57.9 °C, and between -58.7 and -56.9 °C for FIP's (Fig. 6 A). Homogenisation of the carbonic components ($T_h(CO_2)$) in isolated inclusions was to the liquid phase at between 11.8 and 26.9 °C, and between 16.6 and 30.8 °C for FIP's (Fig. 6B). Total homogenisation temperatures ($T_ht$) range between 128 and 245 °C for FIP's (Fig. 5B). Raman microspectrometry revealed the possible presence of magnesite ($MgCO_3$) in one isolated inclusion (CBSqz3A(6)11) with $T_h(CO_2)$ = 23.9°C. Carbonic phases of isolated inclusions consist of $CO_2$ (determined with Raman spectroscopy) ranging between 98 and >99.5 mol%, with $N_2$ and $CH_4$ comprising the remainder of the vapour. Carbonic phases in inclusions in FIP's contain between 32 and >99.8 mol% $CO_2$, <0.5 to 55.5 mol% $N_2$, 0.3 to 35.5 mol% $CH_4$, and <0.1 mol% $H_2S$ (determined with Raman spectroscopy). Salinities for isolated inclusions range between 11.9 and 13.2 wt.% $NaCl_{equiv}$, and between 3.6 and 19.6 wt.% $NaCl_{equiv}$ in FIP's. Bulk densities range between 0.62 and 1.00 g/cm$^3$.

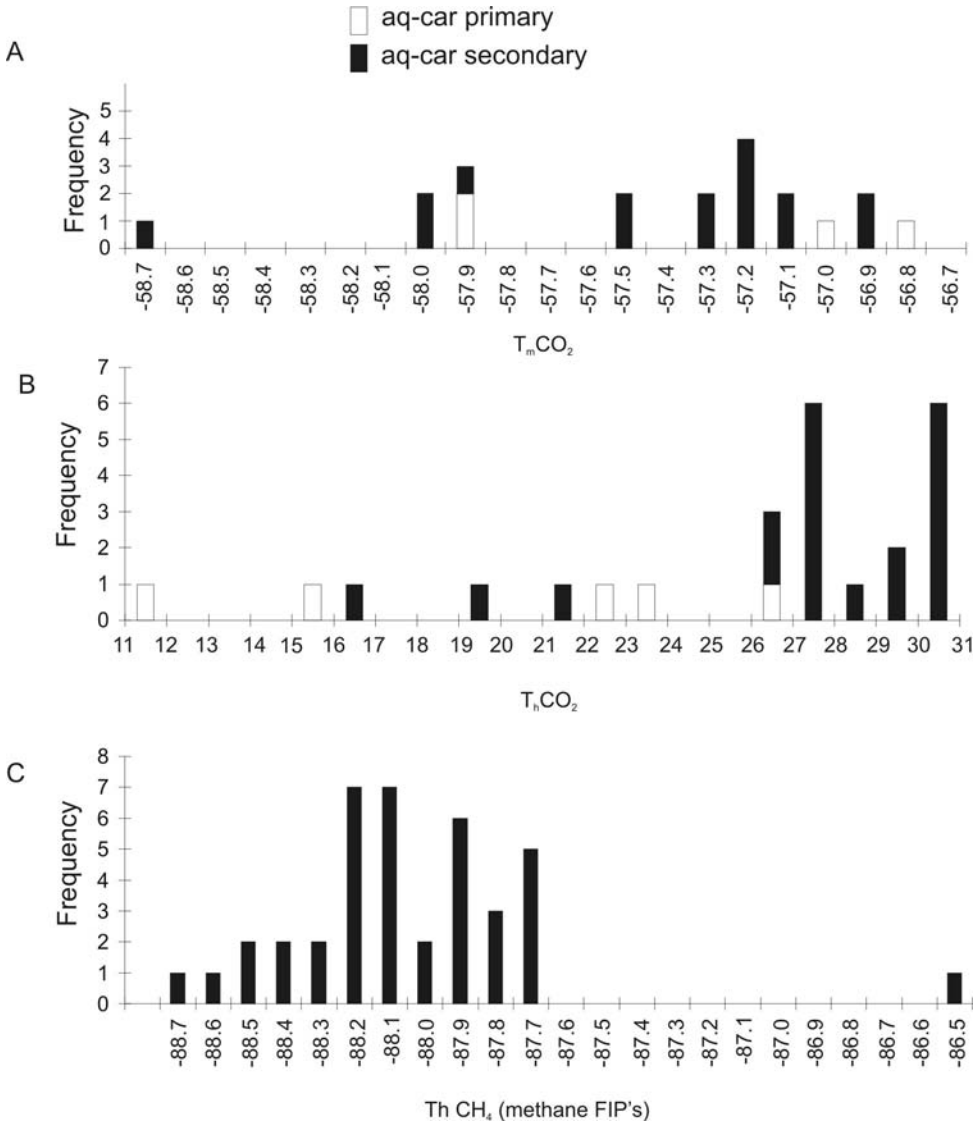


**Figure 6***: A: Histogram of melting of $CO_2$ temperatures ($T_mCO_2$) for all aqueous (aq) and aqueo-carbonic (aq-car) inclusions. B: The distribution in temperatures of $CO_2$ homogenisation for all aqueous and aqueo-carbonic inclusions ($T_hCO_2$). Homogenisation was to the liquid phase. C: Distribution of homogenisation temperatures ($T_hCH_4$) methane inclusions in fluid inclusion planes. Homogenisation for all inclusions was to the liquid phase.*

### *(3) Carbonic methane inclusions*

A distinctive population of fluid inclusion planes comprising numerous methane inclusions was identified, ranging in size between 7-16µm (Fig. 4 J-L). $T_h(CH_4)$ was to the liquid phase at between -88.7 and -86.5 °C (Fig. 6C). Raman spectroscopy indicated the presence of between 6.5 and 7 mol% $N_2$ and between 0.5 and 1 mol% $C_2H_6$. The inclusions are classified according to their phase behaviour as H1-type inclusions with homogenisation as the final phase transition (Van den Kerkhof, 1990).

## INTERPRETATION OF FLUID TYPES

### Early fluids

Isolated inclusions are interpreted as primary inclusions, and therefore represent a fluid that circulated early in the basin history. Salinities of primary aqueous and aqueo-carbonic inclusions range between 11.9 and 23.1 wt% $NaCl_{equiv}$ (Fig. 7A), and final homogenisation temperatures range from 86 to 129°C.

Low-temperature - high-salinity fluids may result from dissolution of evaporites, shale membrane filtration (Graf, 1982), or boiling of a lower salinity fluid. The effect of boiling, or effervescence, whereby the vapour of a high-density fluid is trapped as a low-density fluid (Roedder, 1984), was not observed in this study. The Katanga sequence hosts abundant evaporites in the upper Roan at Mufulira and Konkola, and within the lower Roan (Garlick, 1974). Therefore, the high salinities and low trapping temperatures of isolated aqueous fluid inclusions in this study are best explained by the dissolution of evaporites by circulating connate fluids.

### Later fluids

Secondary inclusions are interpreted to represent fluids that circulated later in the basin history and are characterised by two distinct salinity populations (Fig. 7), namely a low-salinity (~6 wt.% $NaCl_{equiv}$), higher temperature (~140-210 °C) group, and a high-salinity (~18-23 wt.% $NaCl_{equiv}$), lower temperature (~130-160°C) group. The high-salinity group is considered to form from circulating basinal fluids that become increasingly saline and slightly hotter with progressive dissolution of evaporites. The presence of a later, low-salinity, but slightly hotter, fluid may best be explained by devolatilisation reactions during the onset of Lufilian regional metamorphism. Methane, also in secondary inclusion planes, is derived from the decomposition of hydrocarbon organic matter as it passes through the oil window (~60-150°C).

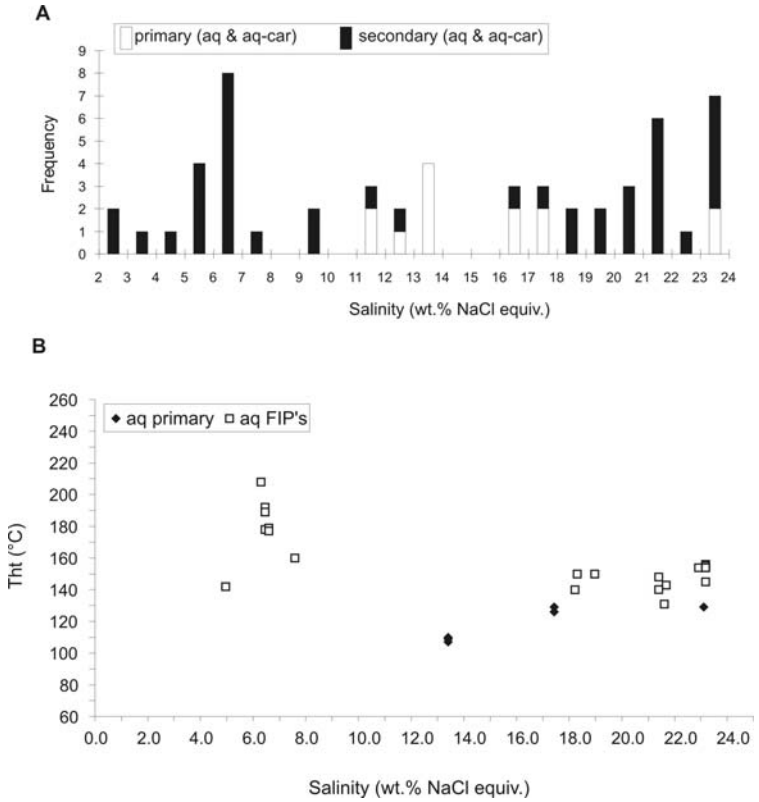


**Figure 7:** *A: Frequency vs salinity (wt.% $NaCl_{equiv}$) for all aqueous and aqueous-carbonic inclusions from isolated and trail populations show a large spread. B: Salinity (expressed in wt.% $NaCl_{equiv}$) vs homogenisation temperatures ($T_ht$) to the liquid phase for primary (black diamonds) and secondary (white squares) aqueous inclusions. Secondary fluid inclusions show two groups in terms of salinity, namely a low-salinity (~6 wt.% $NaCl_{equiv}$) higher temperature (~140-210 °C) group, and a high-salinity (~18-23 wt.% $NaCl_{equiv}$) lower temperature (~130-160°C) group.*

## DISCUSSION

Fluids that immediately post-date stratiform mineralisation are fairly homogeneous in composition and show moderate to high salinities (~12-23 wt.% $NaCl_{equiv}$). Conversely, later fluids exhibit a range in salinities (~6-23 wt.% $NaCl_{equiv}$), compositions, and trapping temperatures. Progressive sediment burial during diagenesis and the resultant heating of connate fluids is evident from Figure 7B, where an early high-salinity fluid evolves to a slightly higher temperature high-salinity fluid. As metamorphism increases, devolatilization reactions result in the production of a fluid of lower salinity, but at higher temperatures.

Isochors plotted on a pressure-temperature diagram give an estimation of P-T conditions during fluid trapping (Roedder, 1984; Reynolds and Goldstein, 1994). Intersection of aqueous and carbonic isochors of homogeneously trapped inclusions constrains the range of P-T conditions applicable to the present study. Isochors for isolated aqueous inclusions were constructed for $T_ht$ ranging between 107 and 129°C, and for $T_ht$ ranging between 131 and 208°C for FIP's. Intersection of aqueous and carbonic isochors in this study constrains the pressure and temperature of fluid inclusion trapping to around 480-800 bar and 130-270 °C (Fig. 8). These data reconstruct the pressure- and temperature conditions of the environment associated with (and immediately post-dating) stratiform copper mineralisation, prior to peak metamorphism.

Previous P-T estimates for mineralising fluids by Kamona (1993), Richards *et al*. (1988a) and Speiser *et al*. (1995) are also plotted on Figure 8. The data by Kamona (1993) constrain the

characteristics of epigenetic carbonate-hosted Pb-Zn mineralising fluids at Kabwe, a mineralisation style that post-dates stratiform copper mineralisation. These fluids are hotter than those detected in the present study. The data by Speiser *et al.* (1995) show the pressure and temperature ranges for conditions associated with epigenetic iron-oxide-copper-gold mineralisation to the northwest of the Copperbelt. This epigenetic-hydrothermal vein-style mineralisation (dated at ~503-512 Ma, Torrealday *et al.*, 1999) post-dates earlier stratiform copper mineralisation and is considered coeval with the peak of regional metamorphism in the Lufilian arc. Pressures and temperatures associated with this style of mineralisation are substantially higher than those documented in this study (Fig. 8). Similarly, the data from Richards *et al.* (1988a) constrain the P-T conditions prevalent during late hydrothermal veining at the Musoshi deposit in the DRC, which is associated with alteration. This event of hydrothermal alteration, dated at ~514 Ma (Richards *et al*., 1988b), is related to peak Lufilian metamorphism and post-dates stratiform copper mineralisation. The range of temperatures attained by Richards *et al*. (1988a) also exceeds those obtained during this study, which constrains, for the first time, the characteristics of a late-diagenetic fluid associated with the environment of stratiform copper mineralisation in terms of composition, salinity, pressure and temperature. This study also documents the character of fluids that evolved subsequent to stratiform mineralisation, and which are associated with the onset of early metamorphism.

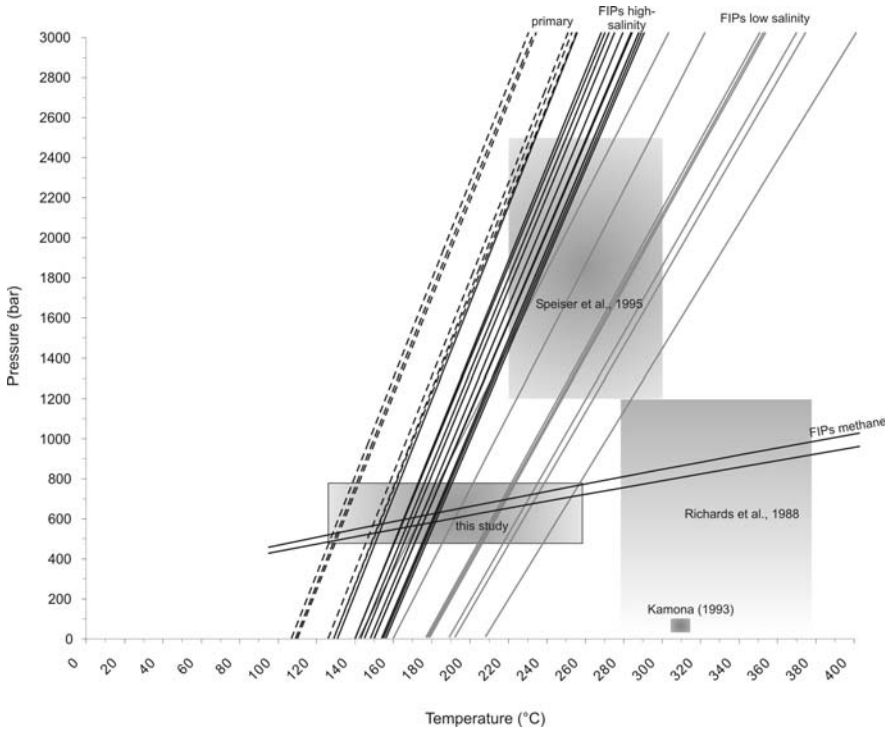


**Figure 8:** *Isochors of primary and secondary aqueous inclusions and methane FIP's. Isochors of primary aqueous inclusions are indicated as dashed lines. Isochors for high salinity FIP's are shown as solid black lines, and sold grey lines for low salinity FIPs. Isochors of methane FIP's are shown as gently sloping solid black lines. Intersection of the aqueous and carbonic (methane) isochors constrain a P-T region of ~480-800 bar and ~130-270°C. Previous studies by Richards* et al.*, (1988a) Speiser* et al.*, (1995), and Kamona (1993) are shown. See text for further details.*

## ACKNOWLEDGEMENTS

Funding for this project was provided by the Economic Geology Research Institute, the National Research Foundation of South Africa, the Centre National de la Recherche Scientifique (CNRS) and the French Embassy, South Africa, and a Hugh E. McKinstry Student Research Award from

the Society of Economic Geologists Foundation. Non-Ferrous Metal Plc is thanked for providing access to the Chambishi deposit. Raman analyses were conducted by Thérèse Lhomme at G2R, UMR 7566, Université Henri Poincaré, Nancy, France. The manuscript was improved by comments from J.M. Huizenga.

## REFERENCES

Armstrong, R. A., Robb, L.J., Master, S., Kruger, F.J. and Mumba, P.A.C.C., 1999. New U-Pb age constraints on the Katanga Sequence, Central African Copperbelt. *Journal of African Earth Sciences*, **28** (4A), 6-7.

Bakker R.J., 1997. Clathrates: Computer programs to calculate fluid inclusion *V-X* properties using clathrate melting temperatures. *Computers and Geosciences*, **23** (1), 1-18.

Bakker, R.J., 2003. Package *FLUIDS* 1. Computer programs for analysis of fluid inclusion data and for modelling bulk fluid properties. *Chemical Geology*, **194**, 3-23.

Bodnar, R.J., 1983. A method of calculating fluid inclusion volumes based on vapor bubble diameters and P-V-T-X properties of inclusion fluids. *Economic Geology*, **78,** 535-542.

Bodnar, R.J. and Vityk, M.O., 1994. Interpretation of microthermometric data for $H_2O$-NaCl fluid inclusions. *In:* De Vivo, B. and Frezzotti, M.L. (eds.), *Short Course of the Working Group (IMA). Fluid Inclusions in Minerals: Methods and Applications*. Virginia Tech, Blacksburg, 117-130 pp.

Boiron, M.C., Essarraj, S., Sellier, E., Cathelineau, M., Lespinasse, M. and Poty, B., 1992. Identification of fluid inclusions in relation to their host microstructural domains in quartz by cathodoluminescence. *Geochimica et Cosmochimica Acta* **56**, 175-185.

Bowers, T.S. and Helgeson, H.C., 1983. Calculation of the thermodynamic and geochemical consequences of non-ideal mixing in the system $H_2O$-$CO_2$-NaCl on phase relations in geological systems: equation of state for $H_2O$-$CO_2$-NaCl fluids at high pressures and temperatures. *Geochimica et Cosmochimica Acta*, **47**, 1247-1275.

Brown, P.E. and Lamb, W.M., 1986. Mixing of $H_2O$-$CO_2$ in fluid inclusions; geobarometry and Archean gold deposits. *Geochimica et Cosmochimica Acta*, **50**, 847-852.

Brown, P E. and Lamb, W.M., 1989. P-V-T properties of fluids in the system $H_2O$ + $CO_2$ + NaCl: new graphical presentations and implications for fluid inclusion studies. *Geochimica et Cosmochimica Acta*, **53**, 1209-1221.

Cahen, L., Snelling, N.J., Delhal, J., Vail J.R., Bonhomme M. and Ledent D., 1984. *The Geochronology and Evolution of Africa*. Claredon Press, Oxford, 512 pp.

Diamond, L.W., 2003. Glossary: Terms and symbols used in fluid inclusion studies. *In:* Samson, I., Anderson, A. and Marshall, D. (eds.) *Fluid Inclusions: Analysis and Interpretation*. Mineralogical Association of Canada Short Course **32**, 363-372.

Fleischer,V.D., 1984. Discovery, geology and genesis of copper-cobalt mineralisation at Chambishi Southeast Prospect, Zambia. *Precambrian Research* **25** (1-3), 119-133.

François, A., 1974. Startigraphie tectonique et minéralisations dans l'Arc cuprifére du Shaba (République du Zaïre). *In:* Barthdolumé P. (ed.). *Gisements Stratiformes et Provinces Cupriféres. Société Géologique de Belgique*, 79-101.

Garlick, W.G., 1961. Chambishi-Nkana Basin. *In:* Mendelsohn, F. (ed.), *The Geology of the Northern Rhodesian Copperbelt.* MacDonald, London, 281-342.

Garlick, W.G., 1974. Depositional and diagenetic environment related to sulphide mineralization, Mufulira, Zambia – a discussion. *Economic Geology*, **69**, 1344 -1351.

Garlick, W.G., 1976. Chambishi. Chapter 6, Geology of the Zambian Copperbelt, V.D. Fleischer, W.G. Garlick, R. Haldane. *In:* Wolf, K.H. (ed), *Handbook of Strata-bound and Stratiform Ore Deposits*, **6**, 249-256.

Goldstein, R.H. and Reynolds, T.J., 1994. Systematics of fluid inclusions in diagenetic minerals. *Society for Sedimentary Geology Short Course* **31**, 199 pp.

Graf, D.L., 1982. Chemical osmosis, reverse chemical osmosis, and the origin of subsurface brines. *Geochimica Cosmochimica Acta*, **46**, 1431-1448.

Jackson, G.C.A., 1932. The geology of the N'Changa district, Northern Rhodesia. *Quarterly Journal of the Geological Society of London*, **88**, 443-515.

John, T., Schenk, V., Scherer, E., Mezger, K., Haase, K. and Tembo, F., 2002. Subduction and continental collision in the Lufulian Arc-Zambezi Belt orogen (Zambia): implications to the Gondwana assembly. *Abstract Volume: 19th Colloquium of African Geology, El Jadida, Morocco*, 19-22 March 2002, p. 188.

Kamona, A.F., 1993. *The carbonate-hosted Kabwe Pb-Zn deposit, Central Zambia*. Ph.D. thesis (unpubl.), Mitteilungen zur Mineralogie und Lagerstättenlehre, RWTH Aachen, 207 pp.

Kampunzu, A.B., Wendorff, M., Kruger, F.J. and Intiomale, M.M., 1998. Pb isotopic ages of sediment-hosted Pb-Zn mineralisation in the Neoproterozoic Copperbelt of Zambia and Democratic Republic of Congo (ex-Zaire): re-evaluation and implications. *Chronique de la Recherche Minière*, **530**, 55-61.

Leroy, J., 1979. Contribution à l'étallonage de la pression interne des inclusions fluids lors de leur décrépitation: *Bull. Minéralogie* **102**, 584-593.

Master, S., Armstrong, R.A., Rainaud, C., Phillips, D. and Robb, L.J., 2004. Provenance ages of the Neoproterozoic Katanga Supergroup (Central African Copperbelt); with implications for basin evolution. *Journal of African Earth Sciences* (this volume).

McGowan, R.R., Roberts, S., Foster, R.P., Boyce, A.J. and Coller D., 2003. Origin of the copper-cobalt deposits of the Zambian Copperbelt: an epigenetic view from Nchanga. *Geology* **31** (6), 497-500.

Mendelsohn, F., 1961a. Metamorphism. *In:* Mendelsohn, F. (ed.), *The Geology of the Northern Rhodesian Copperbelt*. MacDonald, London, 106-116.

Mendelsohn, F., 1961b. Katanga system. *In:* Mendelsohn, F. (ed.), *The Geology of the Northern Rhodesian Copperbelt*. MacDonald, London, 41-54.

Pirmolin, J., 1970. Inclusions fluids dans la dolomite du Gisement stratiforme de Kamoto (Katanga Occidental). *Annales de la Société Géologique de Beligique* **T.93**, 397-406.

Rainaud, C., Master, S. and Robb, L.J., 1999. A fertile Palaeoproterozoic magmatic arc beneath the Central African Copperbelt. *In:* Stanley, C.J. *et al.* (eds.), *Mineral Deposits: Processes to Processing* . Proceedings of the Fifth Biennial SGA Meeting and the Tenth Quadrennial IAGOD symposium, London, 22-25, August 1999, 1427-1430.

Rainaud, C., Master, S., Armstrong, R.A. and Robb L.J., 2003. A cryptic Mesoarchaean terrane in the basement to the Central African Copperbelt. *Journal of the Geological Society, London* **160**, 11-14.

Rainaud, C., Master, S., Armstrong, R.A. and Robb, L.J., 2004. Geochronology and nature of the Palaeoproterozoic basement in the Central African Copperbelt (Zambia and the Democratic Republic of Congo); with regional applications. *Journal of African Earth Sciences*, (this volume).

Richards, J.P., Krogh, T.E. and Spooner, E.T.C., 1988a. Fluid inclusion characteristics and U-Pb rutile age of late hydrothermal alteration and veining at the Musoshi stratiform copper deposit, Central African Copper Belt, Zaire. *Economic Geology*, **83**, 118-139.

Richards, J.P., Cumming, G.L., Kristic, D., Wagner, P.A. and Spooner, E.T.C., 1988b. Pb isotope constraints on the age of sulphide ore deposition and U-Pb age of late uraninite veining at the Musoshi stratiform copper deposit, Central African Copper Belt, Zaire. *Economic Geology*, **83**, 724-741.

Robb, L.J., Master, S., Greyling, L., Yao, Y. and Rainaud, C., 2002. Contributions to the geology and mineralization of the Central African Copperbelt: V. Speculations regarding the "Snowball Earth" and redox controls on stratabound Cu-Co and Pb-Zn mineralization. *In:* C.R. Anhaeusser (ed.), Information Circular, Economic Geology Research Institute, University of the Witwatersrand, Johannesburg, **362**, 38-42.

Robb, L., 2005. *Introduction to Ore-forming Processes*. Blackwell Publishing, Oxford, 373 pp.

Roedder, E., 1972. Composition of fluid inclusions. U S Geological Survey Professional Paper, **440JJ**. 164 pp.

Roedder, E., 1984. *Fluid Inclusions. Reviews in Mineralogy, 12,* Mineralogical Society of America, 646 pp.

Speiser, A., 1994. *Untersuchungen an Flüssigkeitseinschlüssen in Gangquarzen aus der Kansanshi Mine (Solwezi-Area, North-Western District, Zambia).* Diplomarbeit Teil II, Institut für Geologie und Dynamik der Lithosphäre der Geord-Augaust-Universität zu Göttingen, 65 pp.

Speiser, A., Hein, U.F. and Porada H., 1995. The Kansanshi Copper Mine (Solwezi area, northwestern Zambia): geology, wall-rock alteration and fluid inclusions. *In:* Pasava J., Kribek B., and Zak K.K. (eds.), *Mineral Deposits*, Rotterdam, 389-392.

Sweeney, M., 1987. The use of fluid inclusion geochemistry in determining the origin of veins, examples from the Zambian Copperbelt. *Zambian Journal of Applied Earth Sciences* **1**, 18-28.

Sweeney, M. A. and Binda, P.L., 1994. Some constraints on the formation of the Zambian Copperbelt deposits. *Journal of African Earth Sciences*, **19** (4), 303-313.

Torrealday, H.I., Hitzman, M.W., Stein, H.J., Markey, R.,J., Armstrong, R. A. and Broughton D., 1999. Re-Os and U-Pb dating of molybdenite from mineralized veins from the Kansanshi Copper Deposit, Zambia. *In:* Stanley, C.J. *et al.* (eds), *Mineral Deposits: Processes to Processing.* Proceedings of the Fifth Biennial SGA Meeting and the Tenth Quadrennial IAGOD symposium, London, 22-25 August 1999, 1295-1297.

Van den Kerkhof, A.M., 1990. Isochoric phase diagrams in the systems $CO_2$-$CH_4$ and $CO_2$-$N_2$: application to fluid inclusions. *Geochimica et Cosmochimica Acta*, **54** (3), 621-629.

Wendorff, M., 2003. Stratigraphy of the Fungurume Group - evolving foreland basin succession in the Lufilian fold-thrust belt, Neoproterozoic-Lower Palaeozoic, Democratic Republic of Congo. *South African Journal of Geology*, **106**, 17-34.

Zhang, Y.F. and Frantz, J.D., 1987. Determination of the homogenisation temperatures and densities of supercritical fluids in the system NaCl-KCl-$CaCl_2$-$H_2O$ using synthetic fluid inclusions. *Chemical Geology*, **64**, 335-350.

**_____oOo_____**